Journal of Renewable Materials

Tech Science Press

DOI: 10.32604/jrm.2021.015506

ARTICLE

The Accelerated Thermo-Oxidative Aging Characteristics of Wood Fiber/Polycaprolactone Composite: Effect of Temperature, Humidity and Time

Shuang Si, Qian Tang and Xingong Li*

Central South University of Forestry and Technology, Changsha, 410004, China

*Correspondence Author: Xingong Li. Email: lxgwood@163.com

Received: 23 December 2020 Accepted: 25 February 2021

ABSTRACT

This study investigated the characteristics of wood fiber/polycaprolactone composite after an artificial accelerated thermo-oxidative aging treatment. The effect of time, temperature and humidity during the treatment on their mechanical, chemical and morphology properties were evaluated. The composite was prepared from melted wood fibers and modified polycaprolactone by a molding process. A temperature and humidity controllable test chamber was used for the thermo-oxidative aging of the composite. The thermo-oxidative aging caused surface of the composite to be much more rougher and even a few cracks and holes appeared on it. According to the spectra of Fourier Transform Infrared (FTIR) and Gel Permeation Chromatography (GPC), C=O in the molecular chain of polycaprolactone was hydrolyzed and C–O was broken after the aging treatment, which resulted in a reduction in average molecular weight of the composite. Moreover, results showed that the mechanical strength decreased a lot with the increase in time, temperature and humidity, and the effect of temperature and humidity was more significant compared with that of time. Controlling the temperature and humidity during thermo-oxidative aging treatment could accelerate the aging of composite, which provided a quick and effective method for evaluating the aging resistance of the composite.

KEYWORDS

Wood fiber; polycaprolactone; wood plastic composite; thermo-oxidative aging

1 Introduction

With the shortage of timber resources, efforts to develop renewable, degradable, and recyclable materials, that is, green materials, have expanded in recent years. Wood-plastic composites (WPCs) are green composites made by natural wood, straw, bamboo and other plant fibers enhancing or filling the thermoplastics [1]. It not only has the texture and color similar to wood, but also has excellent properties, such as waterproof, high strength, dimensional stability, corrosion resistance and insect resistance [2,3]. Due to these characteristics, WPCs can replace traditional wood and has been widely used in outdoor architecture, garden landscape, automotive industry, packaging and transportation, warehousing, etc. [4]. Polycaprolactone (PCL) is a hydrophobic, semicrystalline and biocompatible polymer [5], which only produces CO_2 and H_2O after biodegradation, and does not cause any pollution to the environment. Because of its good biocompatibility, flexibility, and thermoplasticity, PCL has been widely used to prepare various medical supplies and biological composite [6–8]. The research on PCL-based composite

This work is licensed under a Creative Commons Attribution 4.0 International License, which permits unrestricted use, distribution, and reproduction in any medium, provided the original work is properly cited.

can not only expand the application field of PCL, but also apply the excellent properties to WPCs and promote the development of WPCs industry [9–11].

In spite of good performance and degradability [12–14]. The chemical composition and structure of WPCs will change a lot, and the mechanical properties will decrease during long-term outdoor use. This phenomenon is called aging, caused by the combination of internal and external factors such as heat, oxygen, water, light, microorganisms, chemical media and so on [15]. Aging is an irreversible change, which will lead WPCs to become harder and more brittle [16]. and finally to lose their function. Especially in some areas with high temperature and humidity, the aging phenomenon will be more serious, that begins to attract the attention of researchers.

At present, researches on aging characteristics of WPCs are mainly focused on thermo-oxidative aging [17], photo-oxidative aging [18], biodegradation and some other aging forms. Thermo-oxidative aging, properties of WPCs change in the presence of heat and oxygen, is one of the most common aging phenomena. Thermo-oxidative aging of plastic matrix is the main reason in WPCs [19], because the temperature index of plastics is lower than that of natural fibers such as wood and bamboo. According to previous studies, the thermo-oxidative aging of polymer materials is an autocatalytic oxidation process. So it accords with the free radical reaction mechanism, including the four stages of chain initiation, addition, branching and termination [20]. In order to evaluate the weatherability of WPCs, the most commonly used aging test methods are atmospheric exposure aging test and artificial accelerated aging test [21]. Atmospheric exposure aging is to expose WPCs directly to the outdoor environment so that it will sufficiently affected by the comprehensive factors of the atmosphere. This method is simple and data obtained from it is close to the actual situation [22]. But in this case, an evaluation of the stability against thermo-oxidative aging needs longer periods of exposure and a suitable experimental site. As a contrast, the cycle of artificial accelerated aging test is shorter, and the test factors are controllable. In the development of accelerated aging test methodology, the degradation behavior of the WPCs has to be evaluated without introducing other degradation mechanismsor changing the primary degradation mechanisms [23].

In this study, wood fiber (WF) reinforced PCL composite has been prepared by a certain molding process with fiber as the reinforcing phase and PCL as the matrix. The artificial accelerated thermo-oxidative aging was carried out using a temperature and humidity controllable test chambers. This study was aimed to create an artificial condition to accelerate the thermo-oxidative aging of the WPCs. The effect of temperature, humidity and time on mechanical, chemical and morphology properties were investigated so that we can provide a reference for evaluating the properties of the WPCs in a short time.

2 Experimental

2.1 Materials

Injection molding grade polycaprolactone with a molar mass of 80000 g mol^{-1} was obtained from Shenzhen Huixin Plastic Chemical Co., Ltd., Shenzhen, China. The melting point and melt flow rate for the PCL is 60°C and 7.3 g $(10\ min)^{-1}$, respectively. Plant fibers of poplar (Populus L) with a flour size of 30–60 mesh was purchased from Jiangsu province. A vacuum drying oven was used to dry the fibers. A silane coupling agent (KH550, Hunan Huihong Reagent Co., Ltd., Hunan, China) was used as modifier to improve interfacial compatibility of the WPCs. All chemical agents used in this study were of analytical grade and used without further purification.

2.2 Preparation of the WPCs

Composite of wood fibers containing 40% were prepared according to the route was shown in Fig. 1. The KH550 was dissolved in absolute ethanol at a weight percentage of 1.5% of wood fibers to prepare a solution. The prepared modified solution was uniformly mixed with the PCL particles. And then the PCL

was sent to a vacuum oven at 40°C for 10 h until that all the ethanol was volatilized. The modified PCL particles and fibers were melt-blended in an open two-roll kneader at 100°C for 15 min to obtain a flake mixture, which was then pulverized into granular mixture by a crusher. A single-layer thermocompressor was used to mold the granular mixture into the WPCs at a density of 1.2 g cm^{-3} in a tailor-made mould (250 mm × 250 mm × 6 mm). The hot pressing conditions are as follows: Hot pressing pressure is 10 MPa, time is 20 min and temperature is 100°C, respectively.

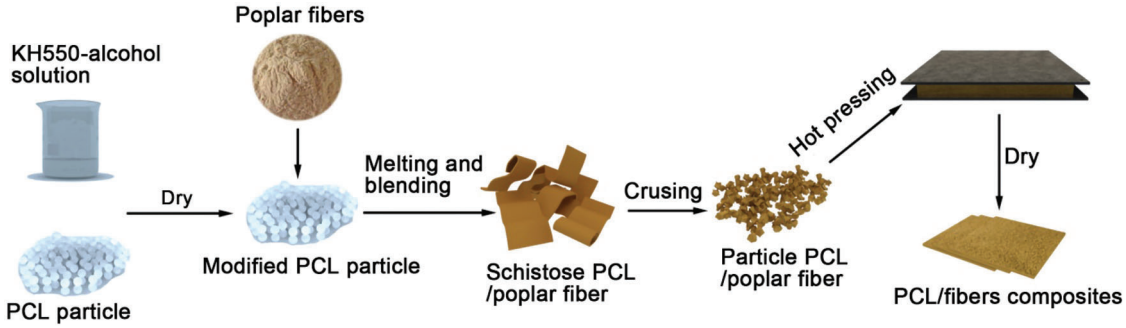

Figure 1: Experimental flow of wood fibers and modified PCL for producing the WPCs

2.3 Thermo-Oxidative Aging Treatment

The WPCs prepared above were sawed into standard test piece by precision panel saw, and then the test piece was placed in a temperature and humidity controllable test chamber for thermo-oxidative aging treatment, the humidity was 75%, and the temperature inside the chamber was set at 60°C. The aging time was: 2 h, 4 h, 8 h, 16 h, 24 h, 48 h, 72 h, 96 h, 120 h, 144 h. After a complete thermo-oxidative aging cycle, the test piece was taken for characterization.

To study the effect of temperature on WPCs, the standard specimens of WPCs were subjected to thermo-oxidative aging treatment. The conditions for thermo-oxidative aging treatment are as follows: The aging time and humidity have always been 72 h and 75%, and the temperature was 50°C, 60°C, 70°C, 80°C, 90°C, respectively. After the thermo-oxidative aging treatment, took out the test piece for testing and characterization.

Same as above, to study the effect of humidity on WPCs, the standard specimens of WPCs were subjected to thermo-oxidative aging treatment. The conditions for thermo-oxidative aging treatment are as follows: The aging time and temperature have always been 72 h and 60°C, and the humidity was 65%, 75%, 85%, 95%, respectively. After the thermo-oxidative aging treatment, took out the test piece for testing and characterization.

2.4 Scanning Electron Microscopy (SEM)

The surface morphology of WPCs after different time aging was observed using a scanning electron microscopy (Quanta 450, Waters, America). Samples were prepared by cutting a small piece of sample and sputter-coating with thin gold layer to provide adequate conductivity.

2.5 Water Vapour Absorption

Untreated WPCs were dried in a vacuum oven at 50°C and tracking the weight over time to measure the oven-dry weight. And then a temperature and humidity controllable test chamber was used for thermo-oxidative aging treatment. Measure the original weight and oven-dry weight of the treated WPCs. The hygroscopicity rate (W) was calculated using the following Eq. (1).

$$W = \frac{M_3 - M_4}{M_1 - (M_2 - M_4)} \times 100\% \quad (1)$$

where M_1 and M_2 in Eq. (1) are the original weight and oven-dry weight of untreated WPCs; M_3 and M_4 are the original weight and oven-dry weight of the treated WPCs, respectively.

2.6 X-ray Photoelectron Spectroscopy (XPS)

An X-ray photoelectron spectrometer (Escalab 250 XI, Thermo Fisher, America) was used to analyze the changes in the chemical composition of the WPCs surfaces before and after aging. The sample was cut into a piece of 5 mm × 5 mm × 3 mm by a blade, polish the black side with sandpaper. The sample was adhered to the aluminum foil with a conductive tape, and then adhered to the sample stage. The monochromatic AlKa target is an X-ray excitation source with a power of 200 W and a beam spot of 650 μm, and the energy analyzer has a fixed transmission energy of 20 eV. The surfaces were investigated for the elemental presence of carbon and oxygen. The ratio of atomic percent of C element and O element can be expressed by Eq. (2).

$$\frac{n_i}{n_j} = \frac{I_i/S_i}{I_j/S_j} \quad (2)$$

where n_i and n_j in Eq. (2) are the concentration of C and O; I_i and I_j are the specific line intensity (peak area) of C and O; S_i and S_j are factor of sensitivity of C and O.

2.7 Fourier Transform Infrared Spectrometry (FTIR)

10 ml of chloroform was used to dissolve 10 mg of sample. Absorb 1 ml of the mixture and filter through an organic filter, and collect the supernatant and droplet on a sheet of potassium bromide. A commercial Fourier transform infrared spectrometer (IRAffinity-1, Shimadzu Corporation, Japan) was used to characterize the change of internal chemical groups in WPCs before and after aging. The spectra was recorded from an accumulation of 128 scans at a 4 cm^{-1} resolution over the regions of 4000–400 cm^{-1}.

2.8 Gel Permeation Chromatography (GPC)

0.3 g of the WPCs sample was dissolved in 20 ml of chloroform, and then filtered through an organic filter, collect the filtered liquid. The gel column type was the PL gel 5 μl MIXED-C cross-linked polystyrene and the column temperature was 37°C. Samples were tested at a flow rate of 1.00 ml min^{-1} and the injection volume is 100 μl. The GPC curve obtained by the test can be used to analyze the changes in the molecular weight of WPCs before and after the aging treatment.

2.9 Mechanical Properties Test

A universal mechanics test machine (DSC-R-100) was used to measure the mechanical strength of sample. The specimens were dumbbell-shaped and five tensile specimens were obtained from each sample. The tensile strength of WPCs was measured according to the standard test method GB/T 1040.5-2008 at a tensile rate of 10 mm min^{-1} [24]. And the test of bending strength follows the standard test method GB/T 17657-2013 [25].

3 Results and Discussion

3.1 Morphologies of the WPCs

The surface morphology comparison of the samples after thermo-oxidativeaging for different time is shown in Fig. 2. It can be seen from the figure that the surface of WPCs without aging treatment was relatively smooth, and there were only a small number of cracks and holes. After 8 h of thermo-oxidative aging, the WPCs were much rougher and there was a little exfoliation on the surface. After

thermo-oxidative aging for 24 h, a large number of filamentous fibers appeared on the surface, and the number and size of cracks and holes gradually increased. When the treatment time was prolonged to 144 h, the aging of WPCs was very serious. There were many bulky exfoliations and large size of cracks and holes on the surface. These phenomena indicated that fibers and PCL may fall off from each other during thermo-oxidative aging and resulted in the destruction of bonding interface [26].

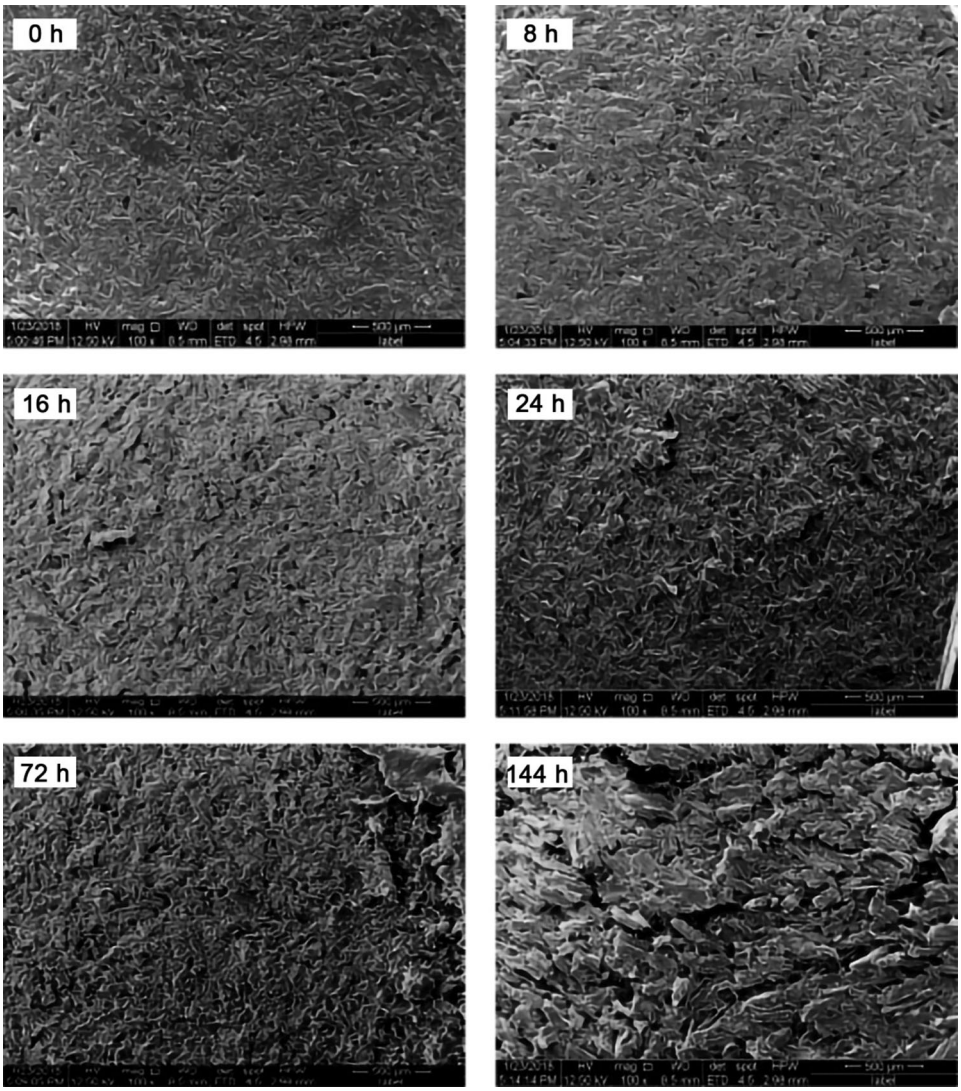

Figure 2: Morphology of the WPCs after thermo-oxidative aging treatment for different time (500 μm)

3.2 Interaction with Water

Fig. 3 shows the hygroscopicity rate of the WPCs after thermo-oxidative aging for different time. In the early stage, the hygroscopic rate changed drastically with the increased time, which was caused by the water vapour absorption of fibers [27,28]. After a period of time, the interface between fibers and PCL was destroyed, and there were cracks and holes appeared on the surface of the WPCs. Water molecules rapidly entered the WPCs through these cracks and holes, resulting in a significant increase in the hygroscopic rate. After 72 h of aging treatment, the hygroscopic rate kept basically stable, because the moisture in the WPCs has reached a relative saturation, that is, a moisture absorption equilibrium state [29,30].

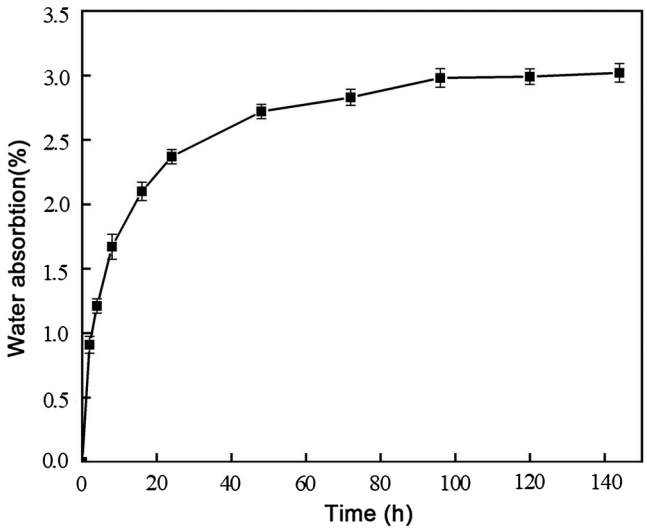

Figure 3: Hygroscopic rate for the WPC s thermo-oxidative aged in 60°C and a humidity of 75%

3.3 Element Analysis

XPS is a research method that uses soft X-rays to excite the electron energy spectrum of a sample. It is mainly used to analyze the surface elements and valence states of samples [31]. In recent years, it has been widely used in chemical composition and valence bond analysis of WPCs [32,33]. Fig. 4 shows the XPS spectrum of the surface of WPCs after thermo-oxidative aging for different time. According to previous studies, the peak near 285 eV represents the C1s and 532 eV represents the O1s [34]. The intensity of the C1s peak did not change a lot with the aging time, but the intensity of the O1s peak depended most significantly on the time. The results of O/C of the WPCs were shown in Tab. 1. As the aging time increases from 2 h to 144 h, the content of C was continued decreased and that of O continued has increased, which caused the result of O/C continue to increase. It indicated that the WPCs has been gradually oxidated and some oxygen-containing functional groups are newly formed on the surface.

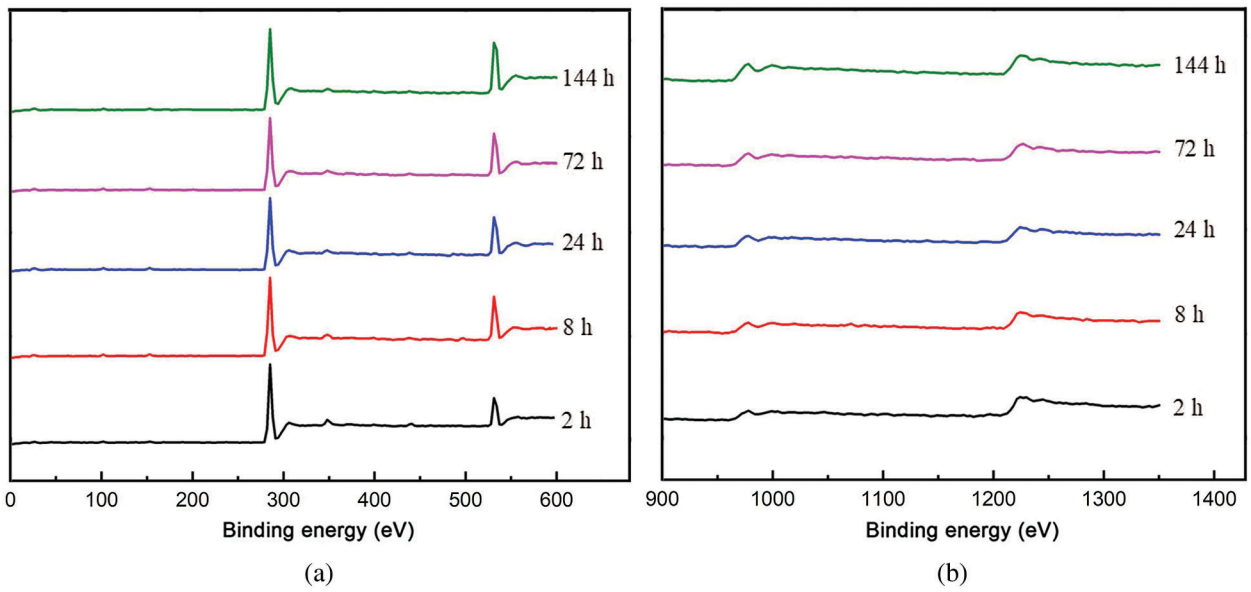

Figure 4: XPS spectra of the WPCs after thermo-oxidative aging treatment for different time

Table 1: Result of O/C of the WPCs after thermo-oxidative aging for different time

Aging time (h)	Element proportion of C (%)	Element proportion of O (%)	Result of O/C
2	83.18	14.48	1.74
8	79.06	17.23	2.18
24	78.33	18.71	2.39
72	76.9	20.22	2.63
144	74.72	22.35	2.99

As previous studies showed that the functional groups on the surface of WPCs mainly included C–C or C–H, C–O or C–OH, and C=O [35,36]. The combined action of heat, water and oxygen caused the ester on the PCL molecular chain to undergo a hydrolysis reaction. With the extension of aging time, the C–O in the PCL molecular chain is continuously broken, to produce PCL with a lower degree of polymerization and a small molecular weight. Hydrolysis reaction generates carboxyl and hydroxyl groups, resulting in an increase in the proportion of O in WPCs [37]. The above is consistent with the characterization results we obtained through FTIR and GPC.

3.4 Fourier Transform Infrared Spectrometry

FTIR spectra of the WPCs treated in different temperature (a) and humidity (b) are presented in Fig. 5. The change of temperature and humidity almost made no difference to the position of characteristic peaks. However, the lower absorption intensity of the C=O stretching vibration peak at 1730 cm^{-1} and the C–O–C stretching vibration peak at 1150–1240 cm^{-1} were observed with increased temperature and humidity [38,39]. It revealed that higher temperature and humidity would lead to the enhancement of water molecular activity, and the hygroscopicity rate of WPCs would increase accordingly. Under the combined influence of water, heat and oxygen, C=O was hydrolyzed, part of C–O in the chain of PCL was broken and formed the molecule with lower degree of polymerization, which resulted in the gradual decrease of C–O and C=O functional groups. In addition, the silanol groups generated by the hydrolyzed silane can form covalent Si–O–C bonds with the poplar fibers. And the absorption intensity of the Si–O–C around 1090 cm^{-1} has also decreased [40]. It was because that fibers and the modified PCL produced dry shrinkage and wet expansion after water vapour absorption, which caused the joint interface between the two to be broken [41]. This conclusion is consistent with the results above.

3.5 Molecular Weight

Gel permeation chromatography (GPC) is a liquid chromatographic method for separating solute molecules according to the volume by controlling the path of polymer solution flowing through the stationary phase [42]. The GPC spectra of WPCs treated in different temperature (a) and humidity (b) are shown in Fig. 6. Width of the peak in GPC curve represents the distribution range of molecular weight, and the earlier the peak appears, the larger the average molecular weight [43]. As shown in Fig. 6, together with the higher temperature and humidity, position of the peak in GPC curve significantly shifted to the right. Combined with the value of average molecular weight shown in Tabs. 2 and 3, it indicated that the thermo-oxidative aging of WPCs led to a gradual decrease in the average molecular weight. At the same time, width of the peak also decreased a lot, demonstrating that the distribution of molecular weight was more concentrated, and PCL with low molecular weight generated. The rise of humidity and temperature caused the molecular chain of PCL to break faster and the average molecular weight to decrease. Controlling the temperature and humidity may effectively accelerate the thermo-oxidative aging of WPCs.

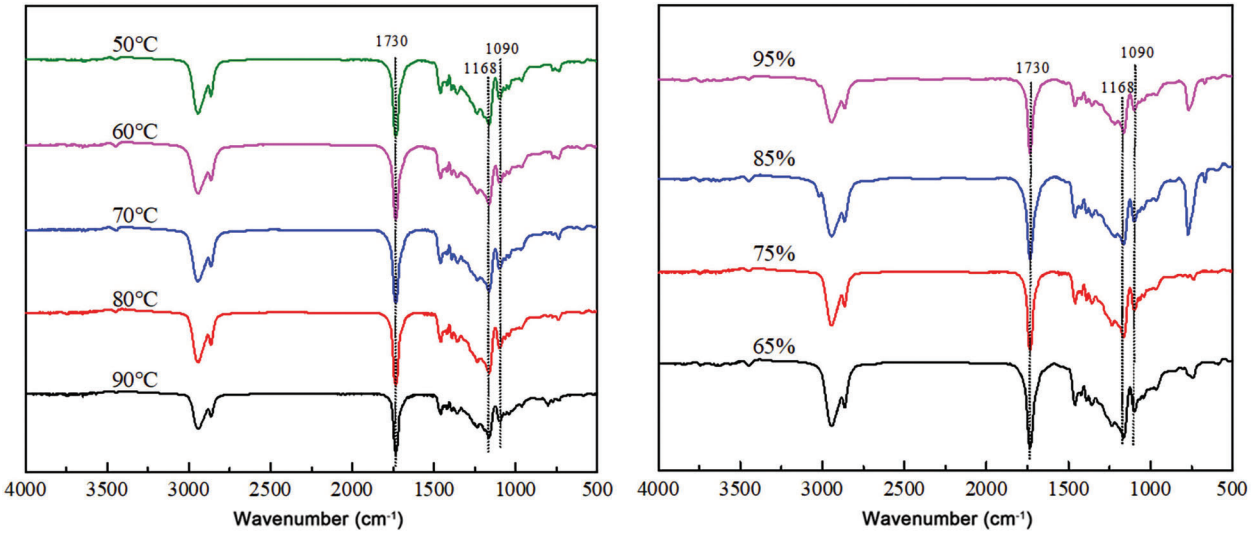

Figure 5: FTIR spectra obtained from thermo-oxidative aged WPCs under different temperature (a) and humidity (b)

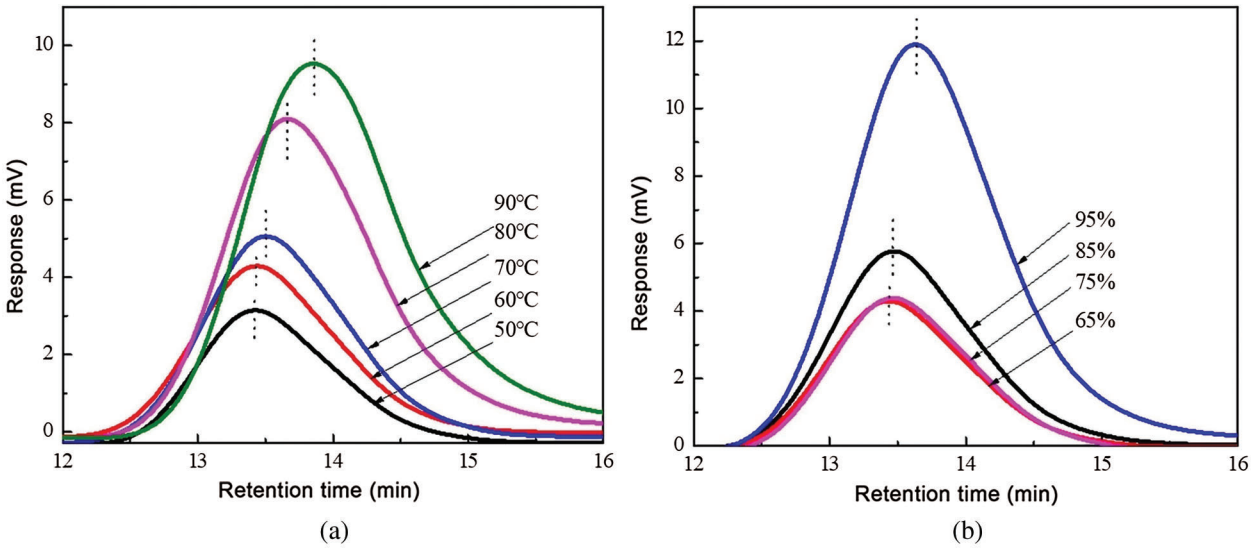

Figure 6: GPC spectra obtained from thermo-oxidative aged WPCs under different temperature (a) and humidity (b)

Table 2: Average molecular weight of the WPCs after thermo-oxidative aging in different temperature

Aging temperature (°C)	Average molecular weight (Mn)	Dispersion coefficient (PD)
50	60587	1.53
60	58872	1.63
70	55002	1.69

Table 3: Average molecular weight of the WPCs after thermo-oxidative aging in different humidity

Aging humidity (%)	Average molecular weight (Mn)	Dispersion coefficient (PD)
65	62593	1.57
75	58872	1.63
85	43591	1.75
95	38627	1.80

3.6 Mechanical Properties

The tensile strength and bending strength of the WPCs after thermo-oxidative aging for different time is shown in Fig. 7. When the time was less than 4 h, the loss of tensile strength and bending strength are small, which suggested that the WPCs can effectively resist thermo degradation in the initial stage of thermo-oxidative aging. Because a small amount of heat gave the molecular chain of PCL the ability to move, some molecular chains were rearranged to form a new crystalline structure [44,45]. Figs. 8 and 9 show the mechanical strength of the WPCs after thermo-oxidative aging for 72 h in different temperature and humidity. When the temperature reached 60°C, the bending strength and tensile strength are reduced to 18.9 MPa and 7.27 MPa and the loss of them added up to 11.46% and 12.19%, respectively. But when the temperature was larger than 60°C, the loss of mechanical strength was faced with a lower speed than that when the temperature is 50–60°C. That maybe because the melting point of PCL was about 60°C [46], so the WPCs softened when the temperature was about 50–60°C after fibers were added into the composite. When the thermo-oxidative aging treatment was carried out at this temperature, the WPCs would partially melt again [47], which could slightly inhibit the decline of mechanical strength. Compared with the aging at different temperature, the loss of mechanical strength of the WPCs continued to accelerate with the increase of humidity. Changing the humidity led to an increase in the saturated moisture absorption of the WPCs, which aggravated the hygroscopic expansion of fiber and PCL. Ultimately, the interface between fibers and PCL was destroyed, and the mechanical properties of WPCs decreased sharply [48]. In addition, a large amount of external heat and oxygen would enter into the WPCs with water [49], which also accelerated the hydrolysis and thermo decomposition of PCL in the WPCs. This result was consistent with the chemical and morphology properties mentioned above. Moreover, it could be seen that temperature and humidity had a more significant effect on mechanical strength than the time, so the speed of thermo-oxidative aging could be accelerated by controlling temperature and humidity.

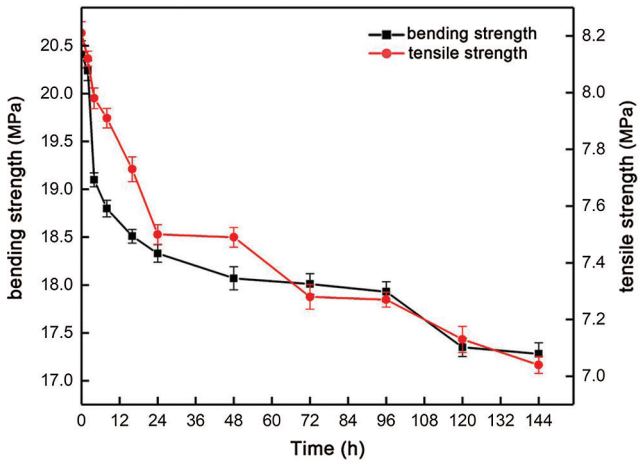

Figure 7: Effect of treatment time on mechanical properties of thermo-oxidative aged WPCs

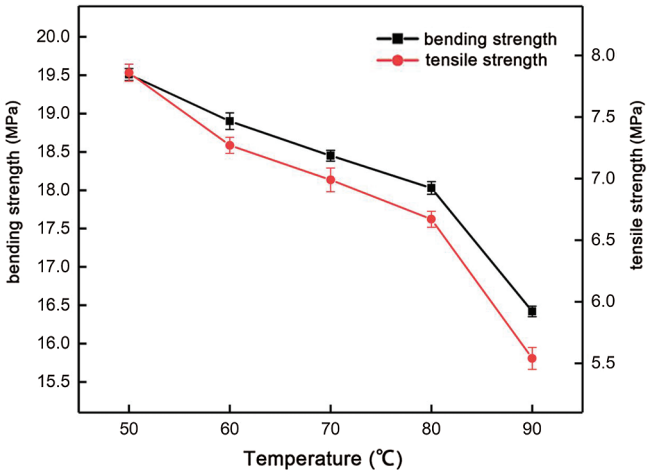

Figure 8: Effect of treatment temperature on mechanical properties of thermo-oxidative aged WPCs

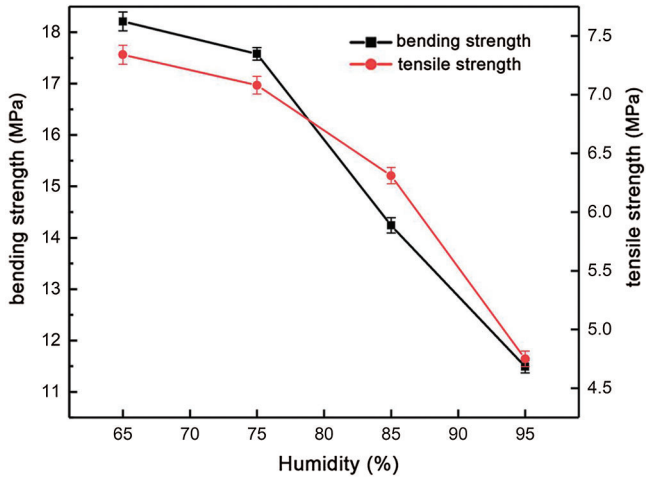

Figure 9: Effect of treatment humidity on mechanical properties of thermo-oxidative aged WPCs

4 Conclusions

In this study, the effect of time, temperature and humidity on the mechanical, chemical and morphological properties of the WPCs was investigated. After the thermo-oxidative aging, PCL degraded under the synergistic influence of water, heat and oxygen. The molecular chain of PCL was broken, and the average molecular weight decreased. In addition, the hygroscopic expansion effect of fibers and PCL caused the joint interface between them to be destroyed, and large cracks and holes appeared on the surface of WPCs. The increase in temperature and humidity lead to a rise in water molecule activity and saturated moisture absorption, and the mechanical strength of WPCs treated in high temperature and humidity were significantly lowered. So by adjusting the temperature and humidity, the speed of thermo-oxidative aging can be controlled, which provided a quick and effective method for evaluating the aging resistance of the WPCs.

Funding Statement: The work was supported by National Key R&D Plan Project (2017YFD0601200), Hunan Key R&D Plan Project (2017SK2334) of College of Materials Science and Engineering, Central South University of Forestry and Technology.

Conflicts of Interest: The authors declare that they have no conflicts of interest to report regarding the present study.

References

1. Ren, D., Yu, Z. X., Zhang, X. X., Wang, H. K., Yu, Y. (2017). Quantitative characterization of the interface between bamboo fiber and polypropylene with pull-out test and nanomechanical imaging. *Journal of Materials Science, 52(3),* 1296–1307. DOI 10.1007/s10853-016-0425-3.
2. Murayama, K., Ueno, T., Kobori, H., Kojima, Y., Suzuki, S. et al. (2019). Mechanical properties of wood/plastic composites formed using wood flour produced by wet ball-milling under various milling times and drying methods. *Journal of Wood Science, 65(1),* 1152. DOI 10.1186/s10086-019-1788-2.
3. Rahman, K. S., Islam, M. N., Ratul, S. B., Dana, N. H., Musa, S. M. et al. (2018). Properties of flat-pressed wood plastic composites as a function of particle size and mixing ratio. *Journal of Wood Science, 64(3),* 279–286. DOI 10.1007/s10086-018-1702-3.
4. Ahmad, F., Choi, H. S., Park, M. K. (2015). A review: natural fiber composites selection in view of mechanical, light weight, and economic properties. *Macromolecular Materials and Engineering, 300(1),* 10–24. DOI 10.1002/mame.201400089.
5. Poornima, B., Korrapati, P. S. (2017). Fabrication of chitosan-polycaprolactone composite nanofibrous scaffold for simultaneous delivery of ferulic acid and resveratrol. *Carbohydrate Polymers, 157(6),* 1741–1749. DOI 10.1016/j.carbpol.2016.11.056.
6. Chen, W. M., Shi, S. K., Zhang, J., Chen, M. Z., Zhou, X. Y. (2016). Co-pyrolysis of waste newspaper with high-density polyethylene: Synergistic effect and oil characterization. *Energy Conversion and Management, 112,* 41–48. DOI 10.1016/j.enconman.2016.01.005.
7. Aguirre-Chagala, Y. E., Altuzar, V., León-Sarabia, E., Tinoco-Magaña, J. C., Yañez-Limón, J. M. et al. (2017). Physicochemical properties of polycaprolactone/collagen/elastin nanofibers fabricated by electrospinning. *Materials Science and Engineering: C, 76,* 897–907. DOI 10.1016/j.msec.2017.03.118.
8. Hu, W. W., Wu, Y. C., Hu, Z. C. (2018). The development of an alginate/polycaprolactone composite scaffold for in situ transfection application. *Carbohydrate Polymers, 183(8),* 29–36. DOI 10.1016/j.carbpol.2017.11.030.
9. Sarasini, F., Tirillò, J., Puglia, D., Dominici, F., Santulli, C. et al. (2017). Biodegradable polycaprolactone-based composites reinforced with ramie and borassus fibres. *Composite Structures, 167,* 20–29. DOI 10.1016/j.compstruct.2017.01.071.
10. Khandanlou, R., Ahmad, M. B., Shameli, K., Hussein, M. Z., Zainuddin, N. et al. (2015). Effect of unmodified rice straw on the properties of rice straw/polycaprolactone composites. *Research on Chemical Intermediates, 41(9),* 6371–6384. DOI 10.1007/s11164-014-1746-y.
11. Khandanlou, R., Ahmad, M. B., Shameli, K., Hussein, M. Z., Zainuddin, N. et al. (2014). Mechanical and thermal stability properties of modified rice straw fiber blend with polycaprolactone composite. *Journal of Nanomaterials, 201(7),* 1–9. DOI 10.1155/2014/675258.
12. André, L. C., Montagna, L. S., Santana, R. M. C. (2017). Abiotic and biotic degradation of post-consumer polypropylene/ethylene vinyl acetate: Wood flour composites exposed to natural weathering. *Polymer Composites, 38(3),* 571–582. DOI 10.1002/pc.23615.
13. Altun, Y., Doğan, M., Bayramlı, E. (2016). Flammability and thermal degradation behavior of flame retardant treated wood flour containing intumescent ldpe composites. *European Journal of Wood & Wood Products, 74(6),* 1–3. DOI 10.1007/s00107-015-0996-8.
14. Ibach, R., Gnatowski, M., Sun, G., Glaeser, J., Leung, M. et al. (2018). Laboratory and environmental decay of wood-plastic composite boards: Flexural properties. *Wood Material Science & Engineering, 13(2),* 81–96. DOI 10.1080/17480272.2017.1313311.

15. Moreno, D. D. P., Hirayama, D., Saron, C. (2018). Accelerated aging of pine wood waste/recycled LDPE composite. *Polymer Degradation and Stability, 149(4),* 39–44. DOI 10.1016/j.polymdegradstab.2018.01.014.
16. Gardner, D. J., Han, Y., Wang, L. (2015). Wood–plastic composite technology. *Current Forestry Reports, 1(3),* 139–150. DOI 10.1007/s40725-015-0016-6.
17. Kobayashi, Y., Kobayashi, S. (2016). Accelerated thermo-oxidative aging for carbon fiber reinforced polycyanate under high pressure atmosphere. *Advanced Composite Materials, 26(5),* 451–464. DOI 10.1080/09243046.2017.1312050.
18. Lu, M., Gao, X. W., Liu, P., Tang, H. Y., Wang, F. et al. (2017). Photo-and thermo-oxidative aging of polypropylene filled with surface modified fumed nanosilica. *Composites Communications, 3,* 51–58. DOI 10.1016/j.coco.2017.02.004.
19. Khalil, H. A., Tehrani, M. A., Davoudpour, Y., Bhat, A. H., Jawaid, M. et al. (2013). Natural fiber reinforced poly (vinyl chloride) composites: A review. *Journal of Reinforced Plastics and Composites, 32(5),* 330–356. DOI 10.1177/0731684412458553.
20. Dai, J., Yan, H., Yang, J. J., Guo, J. J. (2017). Evaluation of the aging behavior of high density polyethylene in thermo oxidative environment by principal component analysis. *Key Engineering Materials, 727,* 447–449. DOI 10.4028/www.scientific.net/KEM.727.447.
21. Chen, Y., Stark, N., Tshabalala, M., Gao, J., Fan, Y. (2016). Weathering characteristics of wood plastic composites reinforced with extracted or delignified wood flour. *Materials, 9(8),* 610. DOI 10.3390/ma9080610.
22. Friedrich, D., Luible, A. (2016). Investigations on ageing of wood-plastic composites for outdoor applications: A meta-analysis using empiric data derived from diverse weathering trials. *Construction and Building Materials, 124(4),* 1142–1152. DOI 10.1016/j.conbuildmat.2016.08.123.
23. Kobayashi, Y., Kobayashi, S. (2017). Accelerated thermo-oxidative aging for carbon fiber reinforced polycyanate under high pressure atmosphere. *Advanced Composite Materials, 26(5),* 451–464. DOI 10.1080/09243046.2017.1312050.
24. GB/T 1040.5-2008 (2008). Plastics: Determination of Tensile Properties, Part 5: Test conditions for unidirectional fiber reinforced composites. China.
25. GB/T 17657-2013 (2013). Test method for physical and chemical properties of wood-based panels and decorative panels. China.
26. Russita, M. B. (2018). Production of palm frond based wood plastic composite by using twin screw extruder. *Materials Science & Engineering Conference Series, 345(1*), 012039. DOI 10.1088/1757-899X/345/1/012039.
27. Wan, Y., Wang, Y. L., Luo, H. L., Dong, X. H., Cheng, G. X. (2002). Moisture absorption behavior of C3D/EP composite and effect of external stress. *Materials Science and Engineering, 326(2),* 324–329. DOI 10.1016/S0921-5093(01)01501-5.
28. Ridzuan, M. J. M., Majid, M. A., Afendi, M., Azduwin, K., Amin, N. A. M. et al. (2016). Moisture absorption and mechanical degradation of hybrid Pennisetum purpureum/glass-epoxy composites. *Composite Structures, 141,* 110–116. DOI 10.1016/j.compstruct.2016.01.030.
29. Dhakal, H. N., Zhang, Z. Y., Richardson, M. O. W. (2007). Effect of water absorption on the mechanical properties of hemp fibre reinforced unsaturated polyester composites. *Composites Science and Technology, 67(7–8),* 1674–1683. DOI 10.1016/j.compscitech.2006.06.019.
30. Babar, A. A., Wang, X. F., Iqbal, N., Yu, J. Y., Ding, B. (2017). Tailoring differential moisture transfer performance of nonwoven/polyacrylonitrile-SiO_2 nanofiber composite membranes. *Advanced Materials Interfaces, 4(15),* 1700062. DOI 10.1002/admi.201700062.
31. Tougaard, S. (2015). Accuracy of the non-destructive surface nanostructure quantification technique based on analysis of the XPS or AES peak shape. *Surface & Interface Analysis, 26(4),* 249–269.
32. Lopez, J. L., Sain, M., Cooper, P. (2006). Performance of natural-fiber-plastic composites under stress for outdoor applications: Effect of moisture, temperature, and ultraviolet light exposure. *Journal of Applied Polymer Science, 99(5),* 2570–2577. DOI 10.1002/app.22884.
33. Stark, N. M., Matuana, L. M. (2007). Characterization of weathered wood-plastic composite surfaces using FTIR spectroscopy, contact angle, and XPS. *Polymer Degradation and Stability, 92(10),* 1883–1890. DOI 10.1016/j.polymdegradstab.2007.06.017.

34. Seah, M. P., Gilmore, I. S., Beamson, G. (2015). XPS: Binding energy calibration of electron spectrometers 5—re-evaluation of the reference energies. *Surface & Interface Analysis, 26(9),* 642–649. DOI 10.1002/(SICI)1096-9918(199808)26:9<642::AID-SIA408>3.0.CO;2-3.
35. Šernek, M., Kamke, F. A., Glasser, W. G. (2004). Comparative analysis of inactivated wood surfaces. *Holzforschung, 58(1),* 22–31. DOI 10.1515/HF.2004.004.
36. Lao, W. L. (2015). *Infrared spectroscopy analysis of biomass content in polypropylene-based wood-plastic composites (Master Thesis)*. China: China Institute of Forestry Sciences.
37. Li, X. G., Zheng, X., Wu, Y. Q., Li, X. J. (2013). Thermal aging properties of bamboo fiber reinforced polylactic acid composite. *Journal of Composites, 30(5),* 101–106.
38. Ibach, R., Gnatowski, M., Sun, G., Glaeser, J., Leung, M. et al. (2018). Laboratory and environmental decay of wood-plastic composite boards: Flexural properties. *Wood Material Science & Engineering, 13(2),* 81–96. DOI 10.1080/17480272.2017.1313311.
39. Kajaks, J., Kalnins, K., Naburgs, R. (2017). Wood plastic composites (WPC) based on high-density polyethylene and birch wood plywood production residues. *International Wood Products Journal, 9(9),* 1–7.
40. Malenab, R., Ngo, J., Promentilla, M. (2017). Chemical treatment of waste abaca for natural fiber-reinforced geopolymer composite. *Materials, 10(6),* 579. DOI 10.3390/ma10060579.
41. Hao, X. L., Zhou, H. Y., Xie, Y. J., Mu, H. L., Wang, Q. W. (2018). Sandwich-structured wood flour/HDPE composite panels: Reinforcement using a linear low-density polyethylene core layer. *Construction and Building Materials, 164(9),* 489–496. DOI 10.1016/j.conbuildmat.2017.12.246.
42. Potthast, A., Radosta, S., Saake, B., Lebioda, S., Heinze, T. et al. (2015). Comparison testing of methods for gel permeation chromatography of cellulose: Coming closer to a standard protocol. *Cellulose, 22(3),* 1591–1613.
43. Cheng, X. P., Zhang, H. B., Hu, J. J., Feng, L. F., Gu, X. P. et al. (2018). Characterization of broad molecular weight distribution polyethylene with multi-detection gel permeation chromatography. *Polymer Testing, 67,* 213–217. DOI 10.1016/j.polymertesting.2018.02.017.
44. Davies, P., Mazéas, F., Casari, P. (2001). Sea water aging of glass reinforced composites: shear behaviour and damage modelling. *Journal of Composite Materials, 35(15),* 1343–1372. DOI 10.1106/MNBC-81UB-NF5H-P3ML.
45. Olakanmi, E. O., Strydom, M. J. (2016). Critical materials and processing challenges affecting the interface and functional performance of wood polymer composites (WPCs). *Materials Chemistry and Physics, 171(2),* 290–302. DOI 10.1016/j.matchemphys.2016.01.020.
46. Thadavirul, N., Pavasant, P., Supaphol, P. (2014). Development of polycaprolactone porous scaffolds by combining solvent casting, particulate leaching, and polymer leaching techniques for bone tissue engineering. *Journal of Biomedical Materials Research Part A, 102(10),* 3379–3392. DOI 10.1002/jbm.a.35010.
47. Jha, K., Tyagi, Y. K., Yadav, A. S. (2018). Mechanical and thermal behaviour of biodegradable composites based on polycaprolactone with pine cone particle. *Sādhanā, 43(9),* 35.
48. Harničárová, M., Mitaľová, Z., Kušnerová, M., Valíček, J., Mitaľ, D. et al. (2017). Analysis of physical-mechanical and surface properties of wood plastic composite materials to determine the energy balance. *Defect and Diffusion Forum, 370,* 78–89. DOI 10.4028/www.scientific.net/DDF.370.78.
49. Wen, Y. Q., Sun, Y. Y., Xu, J. F., Chen, J. B., Zhang, X. X. et al. (2017). Dynamic thermal mechanical behaviors and mechanical properties of reversible thermochromism wood-plastic composite. *Key Engineering Materials, 727,* 571–578. DOI 10.4028/www.scientific.net/KEM.727.571.

Appendix A

Table A1: Related parameters of C element on the surface of composite material after different aging time

Aging time (h)	Peak (eV)	Peak area (CPS.eV)	Sensitivity factor	Atomic fraction (%)
2	284.62	137138.8	1	83.18
8	284.62	160753.4	1	79.06
24	284.62	147919.7	1	78.33
72	284.62	146678.9	1	76.9
144	284.62	164830.1	1	74.72

Table A2: Related parameters of O element on the surface of composite material after different aging time

Aging time (h)	Peak (eV)	Peak area (CPS.eV)	Sensitivity factor	Atomic fraction (%)
2	532.2	63192.96	2.881	14.48
8	532.2	92741.69	2.881	17.23
24	532.2	93493.59	2.881	18.71
72	532.2	102074.3	2.881	20.22
144	532.2	130490.8	2.881	22.35